JOURNAL OF GEOPHYSICAL RESEARCH, VOL. 106, NO. C12, PAGES 31,033–31,044, DECEMBER, 2001

Transport estimates in the Strait of Gibraltar with a tidal inverse model

Burkard Baschek[1] and Uwe Send
Institut für Meereskunde, Kiel, Germany

Jesus Garcia Lafuente
Department of Applied Physics II, University of Malaga, Malaga, Spain

Julio Candela
Centro de Investigacion Cientifica y Educacion Superior de Ensenada, Ensenada, Mexico

Abstract. To estimate the volume transport through the Strait of Gibraltar and to study the spatial structure of the time-variable flow, a varying number of current meter moorings were maintained at the eastern entrance of the strait between October 1994 and April 1998, and was complemented with intensive shipboard measurements during the European Union project Canary Island Azores Gibraltar Experiment (CANIGO). A tidal inverse model is used to merge these data sets in order to investigate the flow at the eastern entrance of the strait. The two-dimensional structure of the tidal flow was described by simple analytical functions. Harmonics with the seven most important tidal frequencies were used as temporal functions. With this model, the tidal currents can be predicted for any time and location at the eastern entrance of the strait, and more than 92% of the variance of the lower layer flow is explained. It was used to remove the tidal currents from the individual measurements and to calculate the mean flow through the strait from the residuals. Combined with a similar inverse model for determining the depth of the interface between Mediterranean and Atlantic water, the volume transport was estimated to be 0.81 ± 0.07 Sv for the upper layer and −0.76 ± 0.07 Sv for the lower layer. The correlation of the tidal currents and the fluctuations of the interface accounts for ~7% of the transport at the eastern entrance.

1. Introduction

In the Strait of Gibraltar the surface flow carries Atlantic water through the contraction of Tarifa Narrows (14-km width) into the Mediterranean Sea (Figure 1). There it is changed in its water mass characteristics by mixing and meteorological influences. After passing through the Mediterranean system, it finally flows back into the Atlantic Ocean at the bottom of the strait and over Camarinal Sill (280-m water depth) as denser and more saline water. This exchange flow also causes a net flux of mass, heat, and freshwater through the Strait of Gibraltar.

However, the mean flow through the Strait of Gibraltar is modified by various processes. These are, in addition to strong tidal currents, mainly currents which are driven by the wind or atmospheric pressure differences between the Atlantic and Mediterranean Sea [*Candela et al.*, 1989]. Also, seasonal [*Garrett et al.*, 1990] and interannual variations seem to be of importance, while on very short timescales the internal bore, an internal wave reaching amplitudes of up to 150 m [*Richez*, 1994], is a dominant process. These flow variabilities have an influence on the exchange transports when they are correlated with the movement of the interface between Atlantic water and Mediterranean water [*Bryden et al.*, 1994].

It is against this background of intense variability on many timescales that the various direct and indirect estimates of the volume transport in the past have to be considered. The values for the lower layer transport vary substantially and are in the range between −0.62 and −1.78 Sv [*Bryden et al.*, 1994]. It is often not clear if the reasons for these differences are due to changes in seasonal or interannual variations, the insufficient spatial or temporal coverage of the measurements, the omission of the effect of interface movement, or an inaccurate estimation of the difference of precipitation and evaporation over the Mediterranean Sea as used in budget models.

To resolve the net inflow into the Mediterranean Sea, as well as the expected low-frequency variability, transport estimates should have an accuracy of at least 0.1 Sv. This represents an observational challenge and requires measurements with high accuracy and good temporal and spatial resolution. Such observations were one aim of the European Union (EU) project Canary Island Azores Gibraltar Experiment (CANIGO) between October 1995 and October 1997. Much of the work presented here was focused on the eastern entrance of the strait with intensive shipboard measurements during several research cruises described in a companion paper [*Send and Baschek*, this issue] (hereinafter referred to as SB) and a substantial number of moorings, which were complemented with U.S.-funded moored measurements.

For the present study these data sets are used to determine

[1]Now at Institute of Ocean Sciences, Sidney, British Columbia, Canada.

Paper number 2000JC000458.
0148-0227/01/2000JC000458$09.00

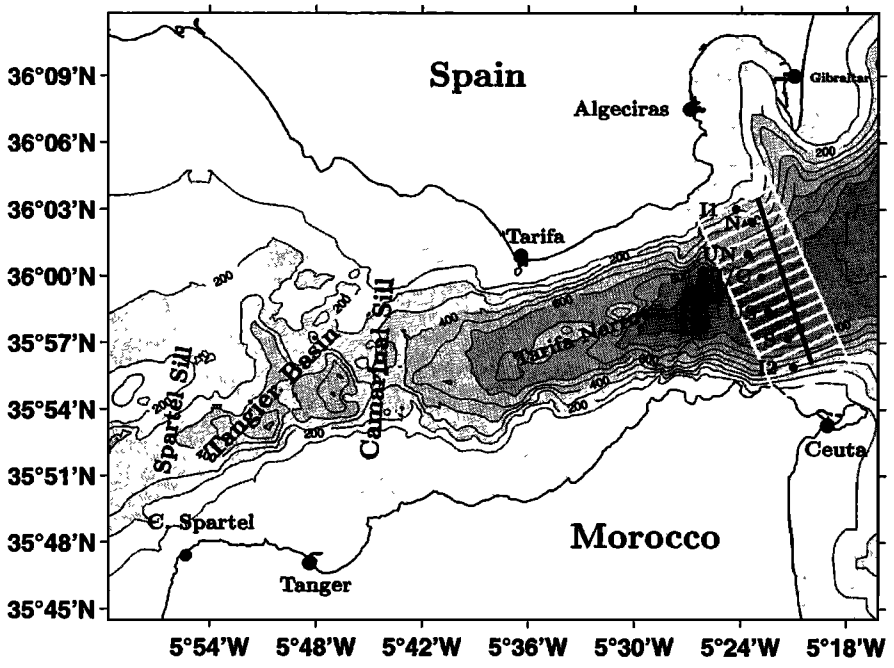

Figure 1. The bathymetry of the Strait of Gibraltar. The vessel-mounted acoustic Doppler current profiler (vmADCP) section at the eastern entrance of the strait is shown by the black line. The dots indicate the positions of the moorings during the intensive phase of the Canary Island Azores Gibraltar Experiment (CANIGO), and the white lines show the positions of the model boxes.

the tidal flow and vertical movement of the interface at the eastern entrance of the Strait of Gibraltar as a function of two space dimensions (cross section) and time. With this model, the mean currents and the volume transports in both layers are calculated, also taking the correlation between tidal currents and the movement of the interface into account.

In the present work a coordinate system is used, which is rotated by +20° relative to Earth coordinates, with the x axis in the along-strait direction (positive into the Mediterranean Sea) and the y axis in the cross-strait direction.

2. Measurements

The oceanographic measurements used in this study and which were carried out during CANIGO mainly focused on monitoring the currents and the depth of the interface between Atlantic and Mediterranean water. The scientific goal of these measurements was to determine the volume transports through the Strait of Gibraltar, to obtain a better understanding of the dynamics and temporal changes of the exchange processes between the Atlantic and Mediterranean Sea, and to design future observing systems [*Send et al.*, 2001].

The flow in the Strait of Gibraltar shows large temporal and spatial variability. To obtain an accurate picture of the currents it is therefore necessary to complement measurements which were carried out at fixed locations for a longer period of time (current meter moorings) with measurements having a good horizontal and vertical resolution (shipboard measurements with vessel-mounted ADCP (vmADCP) and lowered ADCP (lADCP) on sections and time series stations).

The current meter mooring J (Woods Hole Oceanographic Institution (WHOI) and Instituto Hidrografico de la Marina (IHM) and two moorings from the pilot phase of CANIGO, N (University of Malaga) and S (Institut für Meereskunde (IfM), Kiel), were deployed at the eastern entrance of the strait during various intervals between October 1994 and April 1997 (Figure 1) and were equipped with Aanderaa rotor current meters (RCM). The results of these measurements helped to design a mooring array for the intensive phase of CANIGO. It contained the seven current meter moorings I1, I2 Southampton Oceanography Centre (SOC), N, C, S (University of Malaga), and UN, US (IfM, Kiel), which were deployed at the same section from October 1997 to April 1998. They comprised a total of 30 RCMs and one Falmouth Scientific Inc. (FSI) acoustic current meter (see also Figure 8 for a view of the current meter sampling of the section).

In addition, intensive shipboard flow measurements with vmADCP and lADCP were carried out on cross-strait sections at the eastern entrance of the strait during the research cruises *Poseidon* p217 (April 1996) and *Poseidon* p234 (October 1997). Observations of along-strait sections as well as the cross-strait sections at Camarinall Sill and west of the sill are shown in the companion paper SB.

A 150-kHz lowered narrowband ADCP with a beam angle of 20° was used to measure current profiles extending nearly to the bottom of the strait. As it was mounted on the frame of the CTD, simultaneous profiles of temperature and salinity were taken.

The underway current measurements were carried out with a 150-kHz narrowband vessel-mounted ADCP with a beam angle of 30°. The temporal resolution (ensemble length) was 120 or 180 s, and the vertical resolution (bin length) was 16 m, while the vertical range of the ADCP was typically 400 m. The "quasi-synoptic" cross-strait sections at the eastern entrance took ~50 min to complete. One sequence of vmADCP sections over a M_2 tidal cycle is available from cruise p217, and another one is available from cruise p234. For a more detailed description of the shipboard measurements, see also SB.

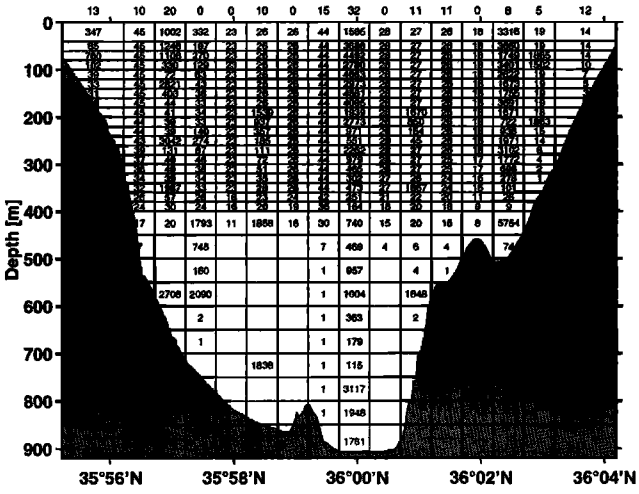

Figure 2. The model boxes at the eastern entrance of the Strait of Gibraltar. The values in the boxes indicate the number of the 2-hour mean values of the along-strait current used in the model calculations. The number of data for the interface depth is shown on top of the figure.

For calculations of the volume transport through the Strait of Gibraltar the depth of the interface between Atlantic and Mediterranean water has to be known. To avoid an influence of the strong seasonal variations of temperature and hence density in the strait, it is usually defined as an isohaline. For the eastern entrance the most appropriate interface definition is the 38.1 isohaline, as discussed in section 4.3. The interface depth was analyzed from CTD data of the research cruises *Poseidon* 217, *Poseidon* 234, *Discovery* 232 (H. Bryden, SOC), and eight cruises with R/V *Odon de Buen* (J. G. Lafuente, University of Malaga), which were all carried out between April 1996 and April 1998. With the help of a time-dependent T-S relation at the central mooring J/C (using the CTD time station over a complete M_2 tidal cycle), it was also determined from expendable bathythermograph (XBT) measurements during the cruise *Poseidon* 234.

3. Inverse Model

Inverse modeling provides a tool to combine these different types of data sets and allows it to extract the temporal as well as the spatial information from the measurements. This means that also the locations with an insufficient temporal sampling (where averages would normally be aliased by tides) can be taken into account and complemented with information from adjacent locations.

All data, which were measured at the eastern entrance of the strait, were sorted into a grid of 16 horizontal and 29 vertical boxes (Figures 1 and 2). The distance between the boxes is ~1 km in the horizontal and 20–50 m in the vertical. To reduce the amount of data, 2-hour mean values were taken before they were sorted into the boxes, yielding a total of ~135,000 data.

Owing to the strong tidal currents, the vertical excursions of the moored current meters sometimes exceeded 150 m. This was taken into account by determining the depth of the instruments at each instant by using the pressure sensors. However, with this method, high currents would be more frequent in deeper boxes, and low currents would be assigned to shallower boxes. Because the data of the single boxes are therefore biased to higher or lower values, a mean value of the boxes cannot be calculated before removing the tidal currents. The same is true for sparsely sampled boxes: First the tides have to be fitted and subtracted before the mean values can be formed. Also, the data of the depth of the isohalines were sorted into the horizontal grid of boxes, and 2-hour mean values were taken subsequently.

3.1. Model Functions

To describe the currents at the eastern entrance of the Strait of Gibraltar as a function of across-coordinate y, depth z, and time t, a combination of simple analytical functions was used, which contain only one of the parameters y, z, or t. They were chosen to reproduce the observed time-variable currents as accurately as possible. With these functions the along-strait component of the current speed is approximately given by

$$u(y, z, t) = A(z) + B(z)C(y)D(t). \tag{1a}$$

With this form, the temporal and spatial dependencies are separated from each other, which allows us to determine the functions A, B, C, and D from the data individually. The vertical flow profile is divided into a mean profile $A(z)$ and a part which describes the flow variability, $B(z)$.

The product of $B(z)$, $C(y)$, and $D(t)$ describes the time- and space-variable flow field. For example, the vertical current profile $B(z)$ is multiplied by $C(y)$ and $D(t)$ and can therefore change with latitude and also time. However, the amount by which B changes is limited by the nature of the chosen functions C and D, which ensures that the calculated flow field does not change too dramatically from one box to the next. Unnatural jumps could otherwise occur owing to the differences of the amount and quality of the available data in the single boxes.

Based on all available measurements from shipboard observations and moorings at the eastern section, the horizontally and temporally constant function of the vertical flow structure $A(z)$ can be approximated with a fourth-order polynomial plus an exponential function with a vertical decay scale of $\gamma_1 = 40$ m and the unknown coefficients a_j:

$$A(z) = a_0 z + a_1 z^2 + a_2 z^3 + a_3 z^4 + a_4 e^{-z/\gamma_1}. \tag{1b}$$

An empirical orthogonal function (EOF) analysis was carried out with vmADCP data from *Poseidon* 217 and *Poseidon* 234 to guide in determining the vertical and horizontal structure of the temporally varying flow field $B(z)$ and $C(y)$. The vertical EOFs were calculated after subtracting the mean flow profile (this part is described by equation (1b) already). Although the two most important vertical EOFs explain most of the variance (56.5% and 35.4%, dashed lines in Figure 3), they were not used for the vertical function $B(z)$, since the profiling range of the vmADCP was limited to the upper 400 m. Because of the insufficient spatial and temporal coverage, also the data from lADCP or moored current meters could not be used to extend the EOFs to the bottom. No lADCP measurements could be carried out during the rapid cross-strait sections, and only a very limited number of moored current meters was available for the same time. Therefore the EOFs were replaced (empirically) with a linear function plus a damped sine and cosine with a length scale of $\kappa = 70$ m and a vertical decay scale of $\gamma_2 = 90$ m (solid lines in Figure 3). The vertical function $B(z)$ with the coefficients b_k is then given by

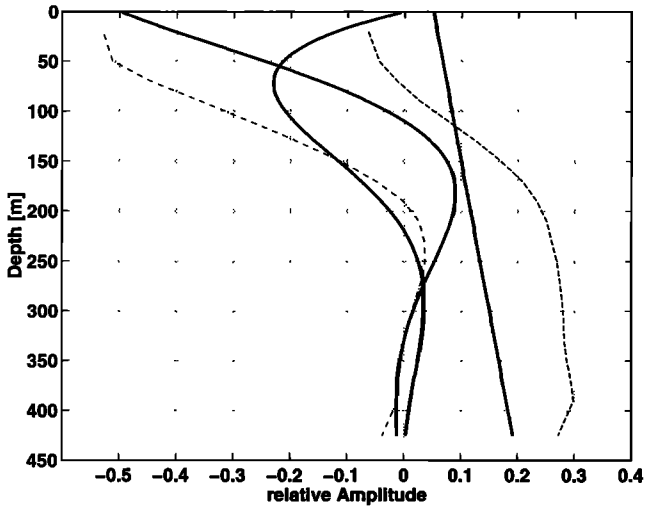

Figure 3. The first (dashed) and second (dash-dotted) vertical empirical orthogonal function (EOF) of the current variance explain 56.5% and 35.4%. The vertical functions, which were used in the inverse model (solid, equation (1c)), together explain 97.8% of the variance.

$$B(z) = b_0 + b_1 z + b_2 \cos(z/\kappa)e^{-z/\gamma_2} + \ldots + b_3 \sin(z/\kappa)e^{-z/\gamma_2}. \quad (1c)$$

This function explains 97.5% of the variance of the vmADCP measurements of both research cruises and is consistent with the deeper variability of the moorings.

Analogously, the horizontal EOFs (61.2% and 12.9% of the variance) were approximated with a polynomial of second order,

$$C(y) = c_0 + c_1 y + c_2 y^2, \quad (1d)$$

explaining 76.2% of the variance of the currents.

The temporal variability is dominated by the tidal currents. The seven most important tidal constituents were determined by a harmonic analysis of the time series of the moored current meters at different locations at the eastern entrance and in different depths. All seven constituents have frequencies of $f > 0.038$ cph (periods $\tau < 25.82h$, Table 1). They were incorporated into the temporal function of the model $D(t)$ by using a combination of sines and cosines,

Table 1. The Angular Speed σ and Period τ of the Tidal Constituents, Which Were Used in the Inverse Model[a]

Tidal Constituent	σ, deg h^{-1}	τ, hours
O_1	13.9430356009	25.82
K_1	15.0410686397	23.93
N_2	28.4397295343	12.66
M_2	28.9841042406	12.42
S_2	30.0000000000	12.00
K_2	30.0821372793	11.96
M_4	57.9682084812	6.21

[a]For the calculation of the interface depth, only the M_2 and S_2 tidal constituents were used.

$$D(t) = d_0 + \sum_{i=1}^{7} [d_{2i-1} \cos(2\pi f_i t) + d_{2i} \sin(2\pi f_i t)]. \quad (1e)$$

It should be noted that the mean flow field in (1a) is given by the first term $A(z)$ but also partly by the second term. The product of d_0 (equation (1e)) with $B(z)$ and $C(y)$ is independent of time and contributes therefore also to the mean flow. However, the inverse model is used to describe the tidal currents but not the mean flow. It is only introduced in (1a) to allow for a better overall fit to the data. The mean flow field can be later calculated by subtracting the modeled tidal components from the measurements and subsequently averaging the data (section 4.1).

The coefficients a_j, plus the combination of the coefficients b_k, c_1, and d_m from (1b)–(1e), gives a total of 185 unknowns which have to be determined. Equation (1a) can be written in the generalized form

$$\mathbf{u} = \mathbf{F}\mathbf{m} + \mathbf{r}, \quad (2)$$

where $\mathbf{F}$ is the matrix which contains the model functions, $\mathbf{m}$ is the vector with the model parameters (the coefficients), and $\mathbf{r}$ are the residuals of the fit. This inverse problem can now be solved to get the estimated model parameters:

$$\mathbf{m}^{est} = (\mathbf{F}^T\mathbf{R}^{-1}\mathbf{F} + \mathbf{P}^{-1})^{-1}\mathbf{F}^T\mathbf{R}^{-1}\mathbf{u}, \quad (3)$$

with the noise covariance matrix $\mathbf{R} = \mathbf{r}\mathbf{r}^T$ and the signal covariance matrix $\mathbf{P} = \mathbf{m}\mathbf{m}^T$.

Once the coefficients $\mathbf{m}^{est}$ are determined, the tidal currents can be calculated for any time t and for any location (y, z) of the two-dimensional cross-strait section of the eastern entrance of the strait by multiplying $\mathbf{m}^{est}$ with the model functions $\mathbf{F}$:

$$\mathbf{u}^{est} = \mathbf{F}\mathbf{m}^{est}. \quad (4)$$

The misfit $\mathbf{r}$ is simply the difference between the measurements u and the modeled currents u^{est}.

Analogously, the depth of the interface ζ was described as a function of latitude y and time t:

$$\zeta(y, t) = R(y)S(t). \quad (5a)$$

The horizontal structure was approximated with a polynomial of second order,

$$R(y) = r_0 + r_1 y + r_2 y^2, \quad (5b)$$

while the temporal fluctuations were again described by a combination of sines and cosines,

$$S(t) = s_0 + \sum_{i=1}^{2} [s_{2i-1} \cos(2\pi f_i t) + s_{2i} \sin(2\pi f_i t)]. \quad (5c)$$

Owing to the considerably smaller amount of available data for the interface depth (top line in Figure 2), only the M_2 and S_2 tidal constituents could be used for the calculations. Also here, the coefficients $\mathbf{n}^{est}$ are determined by

$$\mathbf{n}^{est} = (\mathbf{F}'^T\mathbf{R}'^{-1}\mathbf{F}' + \mathbf{P}'^{-1})^{-1}\mathbf{F}'^T\mathbf{R}'^{-1}\zeta, \quad (6)$$

with $\mathbf{F}'$, $\mathbf{R}'$, and $\mathbf{P}'$ being equivalent to $\mathbf{F}$, $\mathbf{R}$, and $\mathbf{P}$ in (3). The modeled interface depth is given by

$$\zeta^{est} = \mathbf{F}'\,\mathbf{n}^{est}. \quad (7)$$

With the results from (4) and (7) the tidal signal can be removed from the measurements, and the mean volume transport through the strait may be estimated for which the correlation of the currents and the movement of the interface can be taken into account.

3.2. Comparison With Measurements

With the inverse model, the currents corresponding to the seven most important tidal constituents were calculated and subtracted from the observations. The residual currents show which fraction of the flow cannot be reproduced by the model (Figure 4). The standard deviation of the residuals below 200 m is on average less than 12 cm s^{-1}, but above 200 m it is much larger and reaches values of 20–35 cm s^{-1}. This has to be compared to the standard deviation of the measured currents of 35–50 cm s^{-1} in the lower layer and 25–40 cm s^{-1} in the upper layer.

For an analysis of the large variance of the residuals in the upper layer, the time series of the moored current meters (sampled every 0.5 hours) were investigated. The vertical excursions of the instruments were neglected here. After removing the currents corresponding to the seven tidal constituents used in the inverse model, spectra were calculated for instruments deployed in different depths at the center of the eastern entrance of the strait.

The residual currents can then be investigated for long- and short-periodic processes separately. The currents with periods longer than 1.5 days ($\nu < 0.028$ cph) are not included in the inverse model and are here called long-periodic. They comprise long-periodic tidal currents, subinertial currents due to wind and atmospheric pressure difference, as well as seasonal and interannual changes. Analogously, currents with periods smaller than 1.5 days are referred to as short-periodic.

For frequencies $\nu > 0.028$ cph the spectra show pronounced maxima with regular spaces in between them (Figure 5). Their frequencies are approximately given by

$$\nu_i \approx (i + 1)\nu_0, \qquad i = 1, 2, \ldots, \tag{8}$$

with

$$\nu_0 \approx 0.04 \text{ cph} = 1/(24.84 \text{ hours}).$$

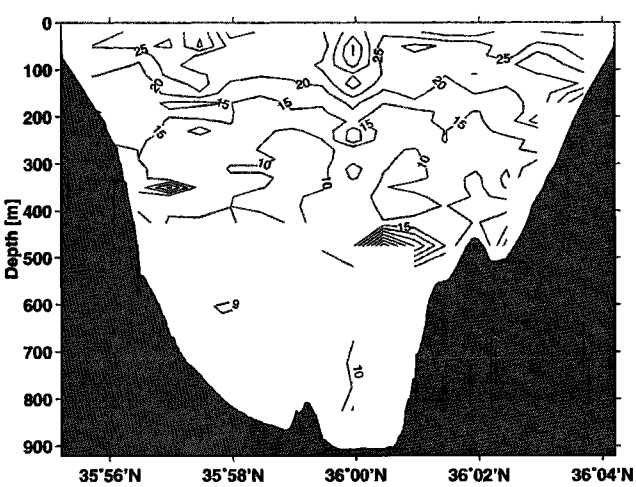

Figure 4. Standard deviation (cm s^{-1}) of the along-strait current residuals, which remain after removing the tidal currents and the mean flow from the observations.

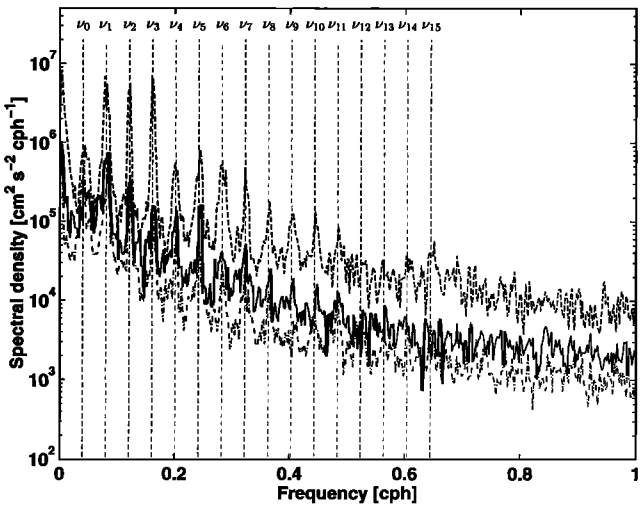

Figure 5. Spectra of the along-strait current residuals of three current meters of mooring J/C (50-m depth, dashed; 145-m depth, solid; 263-m depth, dash-dotted). The dashed lines mark the maxima of the spectra with the corresponding frequencies ν_i (see text).

Because of the high energy of the maxima and their regular spacing, it is likely that they are caused by the currents associated with the internal bore or by nonlinear effects related to the tidal currents. Adding these frequencies into the inverse model does not reduce the residuals, which indicates that there is no stable phase relation to these processes. The reason could be that the time at which the internal bore is released at Camarinal Sill (referred to the tidal cycle) varies and that the advective upper layer currents may be modified by the spring-neap tidal cycle and by subinertial processes. This causes, for example, a variability in the travel time of the internal bore from Camarinal Sill (where it is released) to the east varying between 5 and 9 hours [*Watson and Robinson*, 1990].

For the analysis of the long-periodic residual currents ($\nu <$ 0.028 cph), 1.5 days mean values were taken from the current residuals. Afterwards, EOFs were calculated for boxes with a sufficient amount of data at the center of the eastern entrance of the strait (Figure 6). The two most important EOFs (45.3% and 21.3% of the variance) have their largest amplitudes in the upper 300 m.

The contribution of short- and long-period processes to the residuals as a function of depth is shown in Figure 7, also based on data from the central mooring. It is clear that most of the energy of the supertidal and subtidal processes is concentrated in the upper layer with both parts having similar contributions to the total energy. Because they cannot be reproduced by the inverse model, the variance of the residual currents is much larger in the upper layer. However, in the lower layer more than 92% of the variance of the currents can be explained by the model. It is therefore a useful tool for investigating the lower layer flow and, as will be shown later, for estimating the volume transport of both layers.

4. Results

4.1. Mean Flow

It is still not clear whether the flow through the Strait of Gibraltar is hydraulically controlled or not, or if it may flip

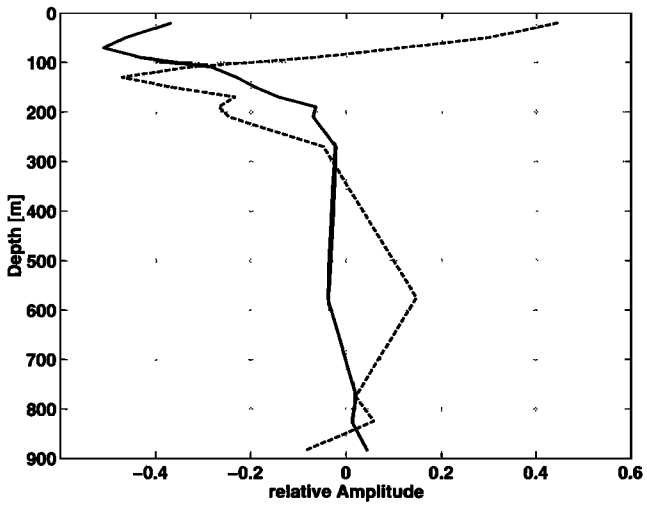

Figure 6. The first EOF (45.3% of the variance, solid) and second EOF (21.3%, dashed) for the long-periodic flow residuals at the central mooring J/C.

from one state to the other [*Garrett et al.*, 1990]. In the theory these two possible states are related to maximal and submaximal exchange [*Armi and Farmer*, 1986; *Farmer and Armi*, 1986], implying that also the currents are different in these two states. It might therefore be necessary to consider two different mean flows, one corresponding to maximal and one to submaximal exchange. However, at this point it was not possible to separate two such states in the analysis of the mean field. Therefore only one average for flows and transports was calculated for the whole period of the measurements, which is a total of four and a half years. Future studies will address the separation issue in more detail.

In the inverse model, the mean flow was described by a temporally constant term (section 3.1). This term was only incorporated into the model to allow for a better fit of the functions varying with latitude and time. However, for accurate calculations of the mean volume transport the structure of the mean flow cannot be sufficiently described by a few simple analytical functions.

Instead, the tidal currents were removed from the measurements, and the mean of the residual currents was calculated for every model box. The spatial gaps due to empty boxes were filled by using an objective analysis. For the covariance matrix, correlation radii of 150 m and 0.04° were chosen. The result is shown in Figure 8b, which compares the result to a tidal average from vmADCP measurements (Figure 8a; see also SB).

The core of the upper layer flow (values up to 80 cm s^{-1}) is located at the surface and is shifted to the south. The lower layer flow has its minimum (maximal outflow) in a depth of 320 m reaching values of about -30 cm s^{-1}. In both layers the currents decrease significantly toward the topography, suggesting that friction plays a role in the strait. The mean position of the 38.1 isohaline is also marked. It is shown below that it separates the inflow and outflow layers at this section.

4.2. Tidal Currents

Synoptic cross-strait current sections can be generated by adding the tidal flow (as calculated by the inverse model) to the mean flow. They highlight the dominating role of the tidal currents in the eastern Strait of Gibraltar (Figure 9). Figure 9 shows a complete M_2 tidal cycle during spring tide with a time step of 2 hours between the single sections. The lower layer flow of the inverse model is periodically reversed by the tidal currents pushing the water back into the Mediterranean Sea. In contrast, in the upper layer the mean flow is too strong and the tidal amplitudes are too small to reverse the flow, and hence it is always directed toward the east. However, observations occasionally show an upper layer flow which is directed toward the west. The absence of such phases in the inverse model suggests that these outflow events are not caused by the linear tides but are due to nonlinear effects or subinertial processes (wind, pressure forcing, etc).

The M_2 tidal constituent is the most dominant one at the eastern entrance of the strait. The amplitude increases from 18 cm s^{-1} at the surface to 42 cm s^{-1} in the lower layer (Figure 10). While there is only little variation of the phases in the lower layer, there is a strong increase in the upper layer from ~150 m to the surface. The mean phase of the upper layer relative to the moon transit in Greenwich is 223.9°, and the one of the lower layer is 148.5° (Table 2).

These results are in good agreement with the ones from *Lafuente et al.* [2000], who published very similar results for the amplitude and phase of the M_2 tide at the eastern entrance. Also, *Candela* [1990] found for the eastern entrance of the strait a decrease in phase of 69° between 54- and 193-m depth and an increase of the amplitude from 21 to 37 cm s^{-1}.

The M_2 tidal constituent of the vertical movement of the interface has a phase of 116.2°. Hence the lower layer flow and the interface are nearly in phase (32.3° difference), while the upper layer flow and the movement of the interface are nearly orthogonal (107.7° difference). For Camarinal Sill, *Bryden et al.* [1994] found a phase difference between upper layer flow and the movement of the interface of 35°–51°. The phase differences will be important for transport estimates, because the correlation of flow and interface movement contributes to the volume transports of both layers.

Also, the S_2 and N_2 tidal constituents have their largest current amplitudes in the lower layer (Table 2), while the O_1, K_1, and M_4 tidal constituents have their maximal values near

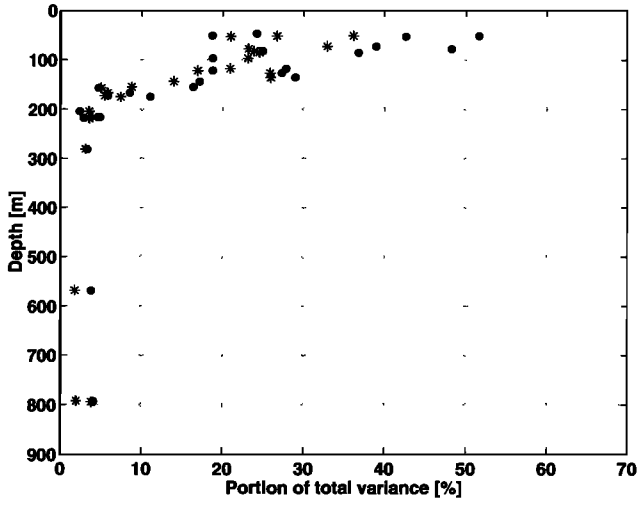

Figure 7. The flow residuals of several current meters at the central mooring J/C, divided into short-periodic ($\nu > 0.028$ cph; asterisks) and long-periodic parts ($\nu < 0.028$ cph; dots). The figure shows the fraction of the variance of each part as a percentage of the total variance of the original time series.

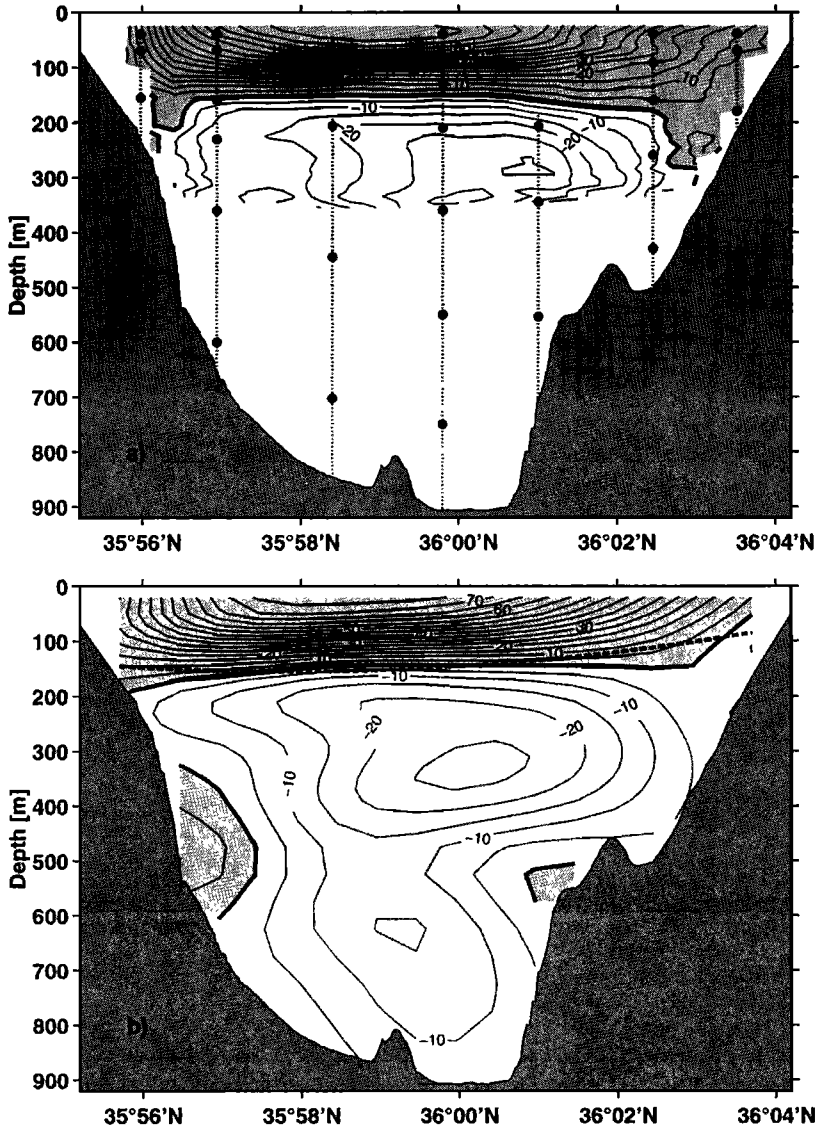

Figure 8. (a) Mean along-strait current (cm s^{-1}) through the eastern entrance of the Strait of Gibraltar from 24 vmADCP sections from *Poseidon* 217 and *Poseidon* 234. The dots show the current meters of the mooring array from the intensive phase of CANIGO. (b) Mean along-strait current (cm s^{-1}) from the inverse model. The mean depth of the 38.1 isohaline is shown by the dashed line.

the surface. The K_2 tidal constituent does not show much difference between both layers. All tidal amplitudes are quite different from the observations from *Bryden et al.* [1994] at Camarinal Sill, implying a strong decrease of the tidal current amplitudes toward the east.

4.3. Transport Estimates

The volume transport through the eastern entrance of the strait was calculated by using the inverse models for the tidal currents and for the depth of the interface (equations (1a) and (5a)), as follows. Synthetic tidal currents were calculated from the inverse model fit for a period of 1 year and were added to the mean flow, which was determined as described in section 4.1. In order to calculate upper and lower layer transports, the depth of the isohaline (which was used as interface definition between both layers) was predicted for every instant from the tidal fit to the isohaline displacement (see section 3.1). With this, the mean flow and the contribution of the correlation between interface movement and tidal currents were determined.

The estimate of the upper and lower layer volume transports thus depends on the choice of the separating isohaline. When, for example, the chosen isohaline lies somewhere in the upper layer, the area of the cross section used for the upper layer calculations is smaller than it should be, and hence also the estimated upper layer transport is too small. At the same time, a part of the upper layer would be ascribed to the lower layer. Since it is flowing in the opposite direction, it also reduces the estimated lower layer transport. It is therefore assumed that the isohaline which maximizes the transports of both layers (Figure 11) is the most appropriate one to use. An isohaline between $S = 38.1$ and $S = 38.15$ seems to be suitable for this, and therefore the 38.1 isohaline is used in this study for further calculations. *Lafuente et al.* [2000] used a similar ap-

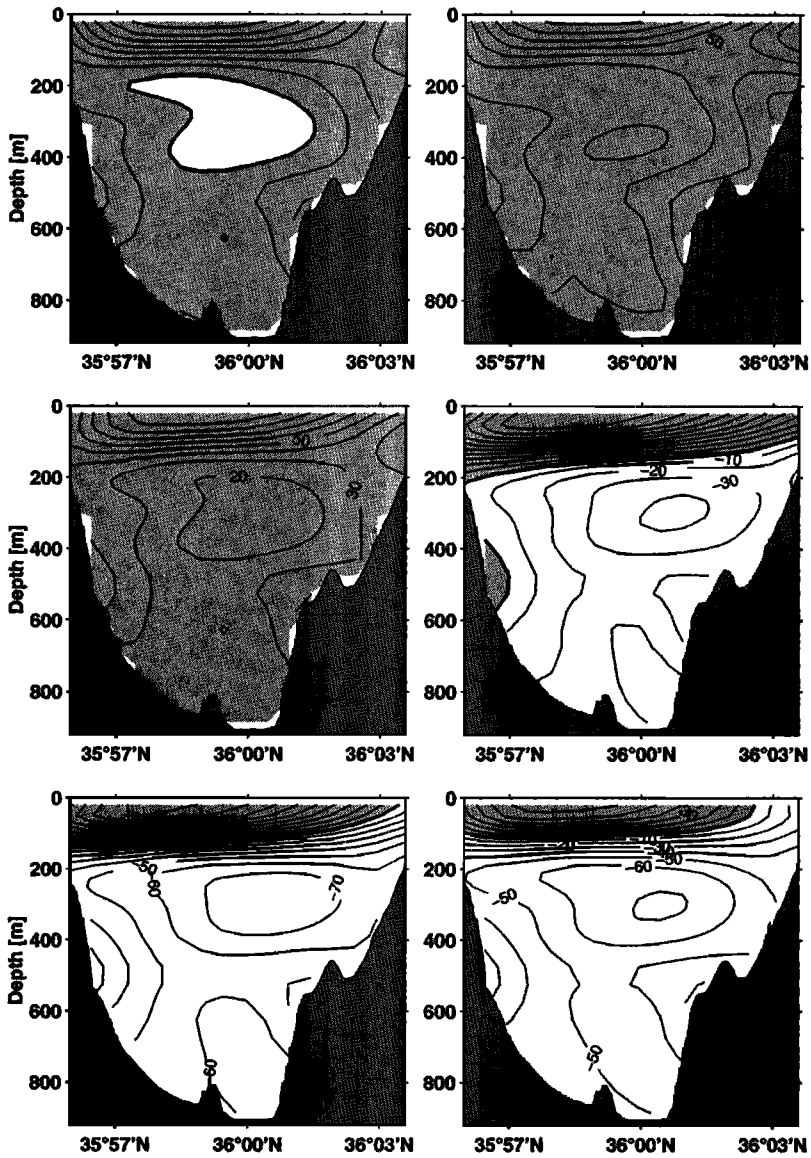

Figure 9. (a–f) Synthetic synoptic sections of the along-strait current (cm s^{-1}) calculated with the inverse model showing several phases of a M_2 tidal cycle during spring tide. The time difference between the single sections is 2 hours.

proach to determine the interface and found the maximal transport for $S = 37.85$.

The volume transport using the 38.1 isohaline is estimated to be 0.81 Sv for the upper layer and −0.76 Sv for the lower layer. Although the difference between these values (the net flow through the Strait of Gibraltar) is in good agreement with the estimated difference of precipitation and evaporation over the Mediterranean Sea [*Bethoux and Gentili*, 1994], it cannot be resolved accurately enough with the inverse model, and the agreement must be partly coincidental.

When the correlation between the tidal fluctuations of the interface and the tidal currents is not taken into account and the transport is calculated for an interface at constant mean depth, the volume transport of the lower layer is larger by ~7% than that for a nonstationary interface. This contribution is far less than the values of more than 45% found by *Bryden et al.* [1994] for Camarinal Sill (and has the opposite sign). The error of the transport estimates, which results from an insufficiently determined depth of the interface, is therefore much smaller in the east than at the sill, owing to the thicker lower layer depth and a smaller interface movement. For accurate transport calculations the interface correlation should still be considered at the eastern entrance, but taking this contribution as a constant will be a good approximation for future measurements.

A comparison with transport estimates from previous publications is difficult, since the direct measurements often suffer from a temporally or spatially insufficient sampling or the vertical movement of the interface was not considered. In addition, error estimates are frequently not given.

The most accurate estimates from direct measurements are probably the ones from *Bryden et al.* [1994] obtained at the sill. They took the vertical movement of the interface into account and determined the transport of the upper layer at the sill to be 0.72 ± 0.16 Sv and the transport of the lower layer to be −0.68 ± 0.15 Sv. Similar values were recently estimated by

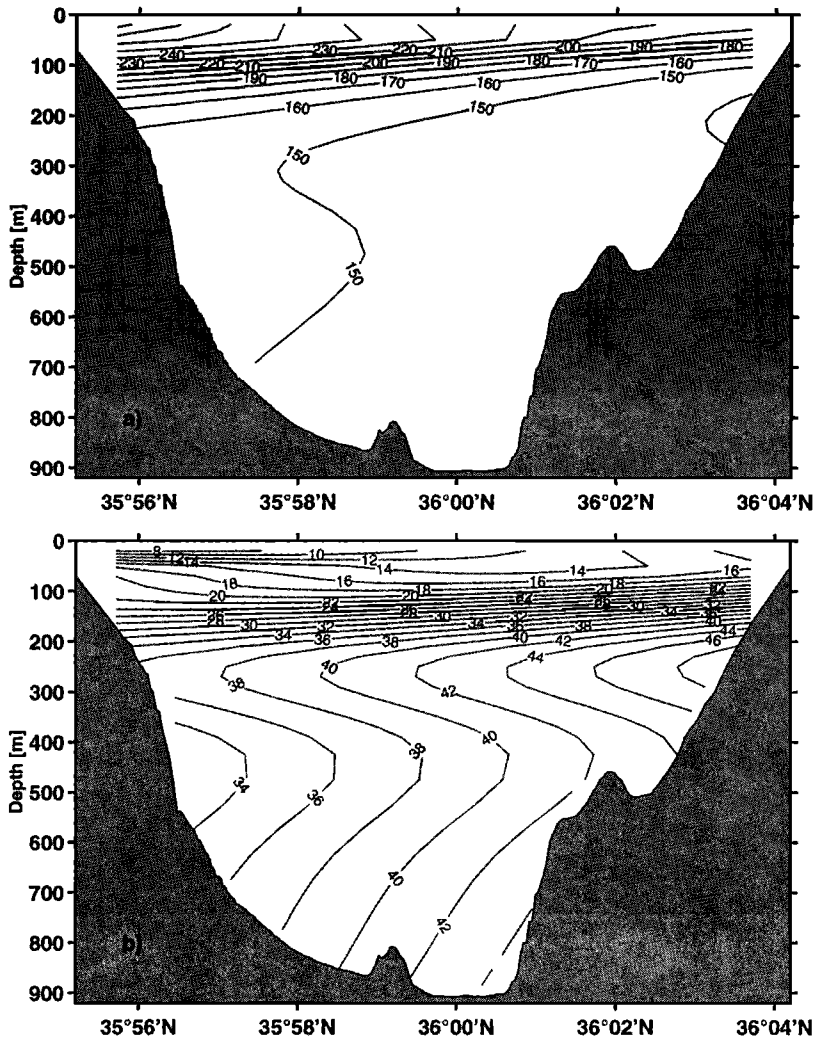

Figure 10. M_2 tidal constituent at the eastern entrance of the Strait of Gibraltar. (a) Phase relative to the moon transit at Greenwich (degrees). (b) Amplitude (cm s^{-1}).

Tsimplis and Bryden [2000] (0.78 Sv and −0.67 Sv) and were also obtained using simple models of the hydraulic control (0.92 Sv and −0.88 Sv [*Bryden and Kinder*, 1991]). All these transport estimates are in reasonable agreement with the results of the present study and lie within the error bars.

Table 2. Amplitude a and Phase ϕ of the Seven Tidal Constituents Computed With the Inverse Model for the Along-Strait Current[a]

Tidal Constituent	Upper Layer		Lower Layer	
	a, cm s^{-1}	ϕ, deg	a, cm s^{-1}	ϕ, deg
O_1	13.0	81.6	6.7	4.1
K_1	12.3	59.1	6.3	−28.3
N_2	3.5	105.7	7.6	75.8
M_2	15.2	223.9	38.3	148.5
S_2	6.8	110.9	11.3	94.9
K_2	2.2	−146.1	2.7	−93.5
M_4	7.3	−86.3	3.2	17.9

[a]Mean values for the upper and lower are calculated. The phase is given relative to the moon transit in Greenwich.

4.4. Error Estimates

The time-mean of the volume transport Q_t of both layers can be calculated from the mean current u_m and the mean area of the cross section A_m, plus the time-dependent parts due to the (seven most important) tidal constituents u'_t, A'_t, short-periodic processes u'_s, A'_s, and long-periodic processes u'_l, A'_l. For each layer this gives

$$Q_t = (u_m + u'_t + u'_s + u'_l)(A_m + A'_t + A'_s + A'_l). \quad (9)$$

The fluctuations in cross section are caused by changes in interface depth or shape. It is assumed that the processes, which contribute to these four parts of the flow, are independent from each other. Then, after averaging over a sufficiently long time, the mixed terms are equal to zero, and we obtain

$$\bar{Q} = \overline{u_m A_m} + \overline{u'_t A'_t} + \overline{u'_s A'_s} + \overline{u'_l A'_l}. \quad (10)$$

The first term $\overline{u_m A_m}$ gives the transport due to the mean currents. The second term $\overline{u'_t A'_t}$ is the result of the tidal fluctuations of the currents and the interface depth which were calculated by the inverse models. The transport values in the previous section were calculated from the sum of these two

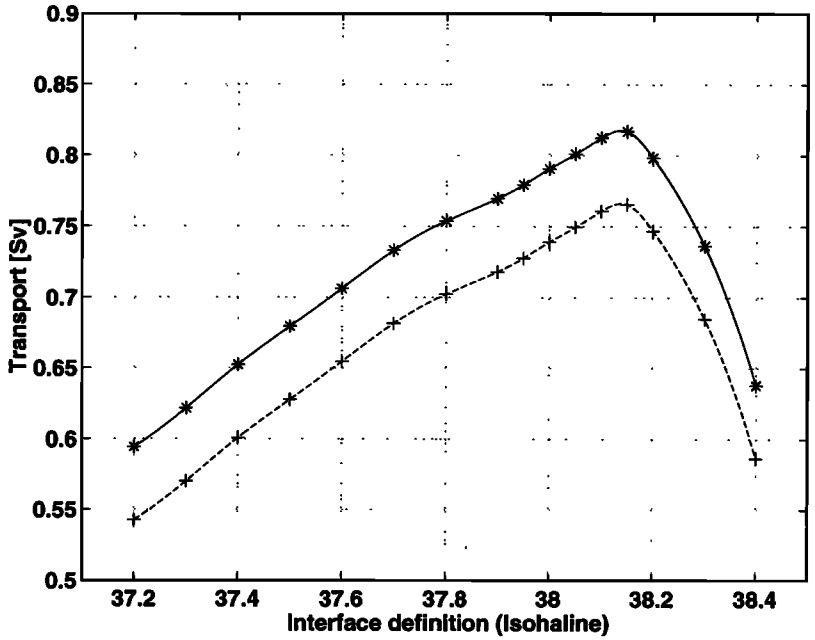

Figure 11. Relation between the interface definition (isohaline) and the calculated volume transport of the upper layer (solid) and lower layer (dashed).

terms. The two remaining terms $\overline{u'_s A'_s}$ and $\overline{u'_l A'_l}$ represent all short- and long-periodic processes which were not included in the model and thus are sources of error. They contain currents and a change of the interface depths related to the remaining tidal constituents, to the internal bore, to other high-frequency contributions, to wind and differences in atmospheric pressure and sea level, as well as to the seasonal cycle. The amplitudes of u'_s and u'_l were estimated by separating the residual currents into a short- and long-periodic part (Figure 7).

The short-periodic deviations of the area of the cross section

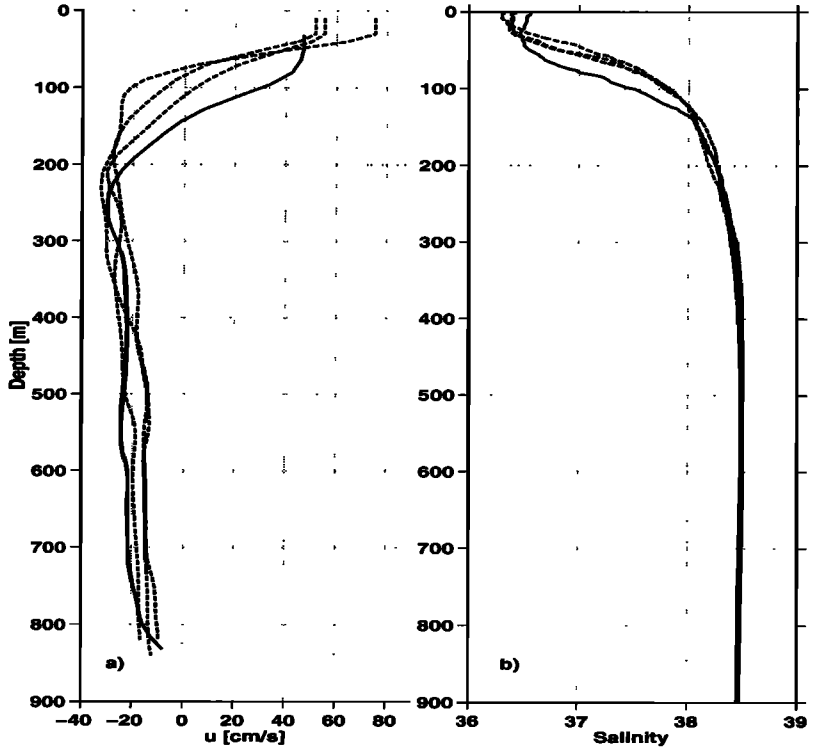

Figure 12. (a) Mean along-strait current profiles averaged over complete M_2 tidal cycles from lADCP measurements from *Poseidon* 217 (April 1996, dashed lines) and *Poseidon* 234 (October 1997, solid line) at the center of the eastern entrance of the strait. (b) Mean salinity profiles from CTD measurements from *Poseidon* 217 (April 1996, dashed lines) and *Poseidon* 234 (October 1997, solid line) at the same location.

Table 3. Mean Values and Error Estimates for the Calculated Mass Transport Through the Strait of Gibraltar[a]

Interface Definition	Transport	Long Periodic	Short Periodic	Error of Measurement	Total Error
$S = 37.4$	$Q_1 = 0.65$	±0.03	±0.04	±0.005	±0.07
	$Q_2 = -0.60$	±0.03	±0.04	±0.014	±0.07
$S = 38.1$	$Q_1 = 0.81$	±0.03	±0.04	±0.005	±0.07
	$Q_2 = -0.76$	±0.03	±0.04	±0.014	±0.07

[a]The transports and its errors are given in sverdrup (Sv).

A_s' were estimated from the residual values resulting from fitting the measured isohaline depths. The long-periodic part A_l' could not be estimated owing to insufficient data. Its order of magnitude was therefore estimated from the lADCP and CTD data from the research cruises *Poseidon* 217 and *Poseidon* 234, which showed a significant difference in the depth of the layer of zero velocity (Figure 12). For the long-periodic fluctuations of the cross section A_l', an error of ±20 m in the layer thickness was therefore assumed.

Assuming perfect correlation of currents and interface movement, conservative error estimates were obtained. Adding also the instrumental measurement errors (Table 3), the total error of the estimated volume transport through the strait for both layers, as derived from (10), is 0.07 Sv rms.

5. Summary

During the EU project CANIGO, intensive shipboard measurements of the flow through the Strait of Gibraltar were carried out and were complemented with moorings in that region. All these data as well as the data of the depth of the interface determined from CTD and XBT measurements were sorted into a grid of 16 horizontal and 29 vertical boxes. These different types of data sets were combined with an inverse model to describe the flow and the depth of the interface with simple analytical functions of two dimensions in space and of time. For the calculation of the currents the seven most important tidal frequencies were considered, and the depth of the interface was determined using the M_2 and S_2 tidal constituents.

In the upper layer the inverse model explains only a small part of the observed currents. The constituents of the flow, which could not be reproduced by the inverse model, are associated with long-periodic ($\nu < 0.028$ cph) and short-periodic ($\nu > 0.028$ cph; e.g., the internal bore) processes, which have their largest amplitudes in the upper 300 m. However, more than >92% of the variance of the flow in the lower layer could be explained with the inverse model.

The mean flow derived from the flow residuals compares well with the mean vmADCP data over 24 sections, with maximal values of 80 cm s^{-1} for the upper layer and −30 cm s^{-1} for the lower layer.

The spatial picture of the dominant M_2 tidal constituent shows an increase of the amplitude with depth and a phase difference between both layers of +75.4° (2.6 hours). The other tidal constituents are less important and generally show a different behavior for both layers.

The interface definition used in this study is the 38.1 isohaline. It is the isohaline for which the values of the calculated volume transport are maximal.

Using the mean currents plus the tidal flow and the interface movement from the inverse model, a mean volume transport of 0.81 ± 0.07 Sv was estimated for the upper layer and −0.76 ± 0.07 Sv was calculated for the lower layer (using an interface definition $S = 38.1$).

The calculated inflow and outflow values lie between the recent direct measurements at Camarinal Sill from *Tsimplis and Bryden* [2000] (0.78 Sv and −0.67 Sv) and from *Bryden et al.* [1994] (0.72 Sv and −0.68 Sv) and the indirect calculations from *Bryden and Kinder* [1991] (0.92 Sv and −0.88 Sv). *Candela* [2001] reports slightly higher estimates (1.01 Sv and −0.97 Sv); however, these are subject to large uncertainties since they are based on a single sill ADCP mooring.

The correlation of the tidal currents and the movement of the interface accounts for ~7% of the volume transport. Although this is far less than at the sill (>45% [*Bryden et al.*, 1994]), it is necessary for accurate transport measurements to consider the movement of the interface also at the eastern entrance of the strait.

The inverse model results are also useful for testing and designing monitoring systems for long-term observations in the Strait of Gibraltar. This was done, for example, for flow observations using cross-strait acoustic transmissions in the Strait of Gibraltar during CANIGO [*Send et al.*, 2001].

Acknowledgments. Most of the current meter moorings and all of the shipboard measurements used in the present work were part of the EU project CANIGO (MAS3-CT96-60). Support for the central J mooring was provided by grant OCE-93-13654 from the U.S. National Science Foundation and contract N00014-94-1-0347 with the Office of Naval Research. We are grateful to Harry Bryden (SOC) for making available the data of the current meter moorings I1 and I2 of the intensive phase of CANIGO and of the hydrographic measurements of the cruise *Discovery* 232. We also thank the captains and the crews of the research vessels *Poseidon* and *Odon de Buen* for their help during the research cruises in the Strait of Gibraltar. We especially thank Bruce Cornuelle (SIO) for his advice on the inverse modeling and the many helpful discussions.

References

Armi, L., and D. M. Farmer, Maximal two-layer exchange through a contraction with barotropic net flow, *J. Fluid Mech.*, *164*, 27–51, 1986.

Bethoux, J. P., and B. Gentili, The Mediterranean Sea: A test area for marine and climate interactions, in *Ocean Processes in Climate Dynamics: Global and Mediterranean Examples*, edited by P. Malanotte-Rizzoli and A. R. Robinson, pp. 239–254, Kluwer Acad., Norwell, Mass., 1994.

Bryden, H. L., and T. H. Kinder, Steady two-layer exchange through the Strait of Gibraltar, *Deep Sea Res.*, *38*, 445–463, 1991.

Bryden, H. L., et al., Exchange through the Strait of Gibraltar, *Prog. Oceanogr.*, *33*, 201–248, 1994.

Candela, J., The barotropic tide in the Strait of Gibraltar, in *The*

Physical Oceanography of Sea Straits, edited by L. J. Pratt, pp. 133–141, Kluwer Acad., Norwell, Mass., 1990.

Candela, J., The Mediterranean water and the global circulation, in *Observing and Modelling the Global Ocean*, edited by G. Siedler, J. Church, and J. Gould, pp. 419–429, Academic, San Diego, Calif., 2001.

Candela, J., et al., Meteorologically forced subinertial flows through the Strait of Gibraltar, *J. Geophys. Res.*, *94*, 12,667–12,679, 1989.

Farmer, D. M., and L. Armi, Maximal two-layer exchange over a sill and through a combination of a sill and a contraction with barotropic flow, *J. Fluid Mech.*, *164*, 53–76, 1986.

Garrett, C., M. Bormans, and K. Thompson, Is the exchange through the Strait of Gibraltar maximal or submaximal?, in *The Physical Oceanography of Sea Straits*, edited by L. J. Pratt, pp. 271–294, Kluwer Acad., Norwell, Mass., 1990.

Lafuente, J. G., J. M. Vargas, F. Plaza, T. Sarhan, J. Candela, and B. Baschek, The tide at the eastern section of the Strait of Gibraltar, *J. Geophys. Res.*, *105*, 14,197–14,213, 2000.

Richez, C., Airborne synthetic aperture radar tracking of internal waves in the Strait of Gibraltar, *Prog. Oceanogr.*, *33*, 93–159, 1994.

Send, U., and B. Baschek, Intensive shipboard observations of the flow through the Strait of Gibraltar, *J. Geophys. Res.*, this issue.

Send, U., P. F. Worcester, B. D. Cornuelle, C. O. Tiemann, and B. Baschek, Integral measurements of mass transport and heat content in straits from acoustic transmissions, *Deep Sea Res.*, in press, 2001.

Tsimplis, M. N., and H. L. Bryden, Estimation of the transports through the Strait of Gibraltar, *Deep Sea Res.*, *Part I*, *47*, 2219–2242, 2000.

Watson, G., and I. S. Robinson, A study of internal wave propagation in the Strait of Gibraltar using shore-based marine radar images, *J. Phys. Oceanogr.*, *20*, 374–395, 1990.

B. Baschek, Institute of Ocean Sciences, 9860 West Saanich Road, Sidney, British Columbia, Canada V8L-4B2.

J. Candela, Centro de Investigacion Cientifica y Educacion Superior de Ensenada, Apdo Postal 2732, Ensenada B.C., Mexico. (jcandela@cicese.mx)

J. G. Lafuente, Department of Applied Physics II, University of Malaga, Campus Teatinos, 29071 Malaga, Spain. (glafuente@ctima.uma.es)

U. Send, Institut für Meereskunde, Ozeanzirkulation und Klima, Düsternbrooker Weg 20, 24105 Kiel, Germany. (usend@ifm.uni-kiel.de)

(Received May 24, 2000; revised July 13, 2001;
accepted July 24, 2001.)